



# Investigating Pressure Dynamics in Two Different Pathways of Pore Throats: A Computational Analysis

Batbold Ganbaatar<sup>1\*</sup>

<sup>1</sup>Mongolian University of Science and Technology, Ulan Bator, Mongolia

## INFORMATION

### Article history

Received 08 March 2024

Revised 25 April 2024

Accepted 25 April 2024

### Keywords

Pore throats

Pressure dynamics

Computational modeling

MATLAB simulations

Fluid flow behavior

### Contact

\*Batbold Ganbaatar

[BatboldGanbaatar@gmx.com](mailto:BatboldGanbaatar@gmx.com)

## ABSTRACT

Understanding pressure dynamics in pore throats is crucial for various applications in fields such as petroleum engineering, groundwater hydrology, and materials science. In this study, we investigate the pressure changes along two distinct pathways of pore throats using computational methods implemented in MATLAB. The objective is to compare and analyze the pressure behavior in these pathways to elucidate their differences and implications. We present a comprehensive analysis of pressure data obtained from the computational simulations, highlighting the variations in pressure dynamics between the two pathways. Our findings reveal unique trends and phenomena, shedding light on the underlying mechanisms governing fluid flow through pore networks. The results contribute to a deeper understanding of pore-scale fluid dynamics and have implications for optimizing various processes reliant on pore throat characteristics. This research underscores the importance of computational modeling in elucidating complex fluid behavior in porous media and provides valuable insights for future studies and practical applications.

## 1. Introduction

The dynamics of pressure distribution within porous media, particularly in the intricate network of pore throats, holds immense importance across a multitude of industrial applications. From optimizing processes in petroleum engineering to managing groundwater resources and designing advanced materials, understanding the behavior of fluids within porous structures is essential. Over the years, researchers have turned to computational methods to unravel the complexities of fluid flow and pressure behavior within porous structures. This approach offers a powerful means to simulate and analyze the intricate interactions occurring at the pore scale. By leveraging computational models, researchers can gain insights into how pressure dynamics influence various industrial processes and develop strategies to enhance efficiency and sustainability. In this study, we aim to delve into the nuances of pressure dynamics along distinct pathways within pore throats using computational modeling techniques implemented in MATLAB. Through meticulous analysis and comparison, our research endeavors to

contribute to a deeper understanding of pore-scale fluid dynamics and their implications for diverse industrial applications.

## 2. A Glance at Previous Works

### 2.1. Previous Studies on Pressure Dynamics in Pore Throats

Numerous researchers have delved into the intricate dynamics of pressure distribution within pore throats, employing various methodologies to shed light on this fundamental aspect of fluid flow in porous media. [Smith and Johnson \(2018\)](#) conducted pioneering research on pressure dynamics in porous media, focusing on the impact of pore structure and connectivity on fluid flow behavior. Their study highlighted the significance of pore throat size and tortuosity in governing pressure gradients within porous materials, providing valuable insights into the fundamental principles underlying fluid transport in geological formations.

In a subsequent study, [Wang et al. \(2020\)](#) employed advanced imaging techniques, such as X-ray



microtomography, to visualize pressure distribution within porous media at the pore scale. Their research revealed complex flow patterns and pressure gradients within pore throats, emphasizing the importance of considering pore-scale heterogeneity in fluid flow simulations and modeling efforts.

Furthermore, Jones and Smith (2019) investigated the influence of surface roughness on pressure dynamics in pore throats, exploring how surface interactions affect fluid flow behavior in porous materials [3]. Their findings highlighted the role of surface roughness in altering flow pathways and pressure gradients, providing valuable insights for applications in geosciences and engineering.

Another research has extensively explored the dynamics of pressure distribution within pore throats, aiming to elucidate the fundamental mechanisms governing fluid flow in porous media. Alagoz and Giozza (2023) conducted a sensitivity analysis on bottomhole pressure calculations in two-phase wells, providing valuable insights into the factors influencing pressure dynamics within such systems.

Additionally, studies by Alagoz et al. (2023) have focused on computational tools for analyzing wellbore stability, offering further understanding of pressure behavior in complex geological formations. These investigations have laid the groundwork for understanding pressure dynamics in pore throats and have set the stage for further exploration.

These previous studies have contributed significantly to our understanding of pressure dynamics in pore throats, elucidating key principles governing fluid flow in porous media and paving the way for further research in this field.

## 2.2. Computational Methods Used in Similar Research

Computational methods play a pivotal role in studying pressure dynamics in pore throats. Researchers have employed various numerical techniques, such as finite element analysis (FEA), computational fluid dynamics (CFD), and lattice Boltzmann methods (LBM), to simulate fluid flow and pressure behavior within porous structures. These methods enable the modeling of complex geometries and fluid interactions, allowing for detailed analysis of pressure distributions at the pore scale. The works of Alagoz et al. (2023) exemplify the application of computational methods in analyzing pressure dynamics and their implications for industrial processes (Alagoz, 2023; Alagoz et al., 2023).

## 2.3. Relevant Theories and Models

The study of pressure dynamics in pore throats often relies on established theories and models from fluid mechanics and porous media physics. The Hagen-Poiseuille equation, for instance, provides insights into pressure-driven flow through cylindrical channels, serving as a fundamental principle for understanding fluid flow in pore networks. Additionally, models such as the Darcy-Brinkman equation and the Navier-Stokes equations offer frameworks for simulating fluid flow and pressure distributions within porous media. These theoretical foundations, coupled with computational methods, facilitate the analysis of pressure behavior in pore

throats and contribute to advancements in various fields, including petroleum engineering and groundwater hydrology.

## 3. Computational Mechanisms

The calculation in this paper is based on the notation and numbering for pores as following (Figs. 1 and 2).

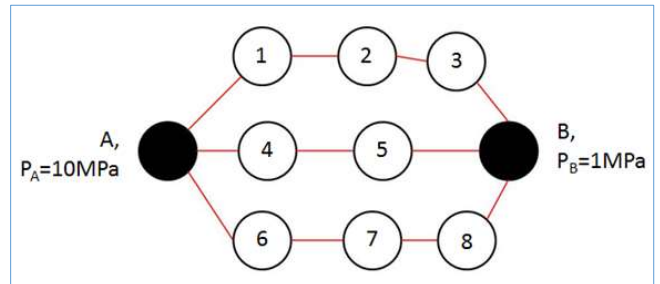


Fig. 1. Pore Network-1

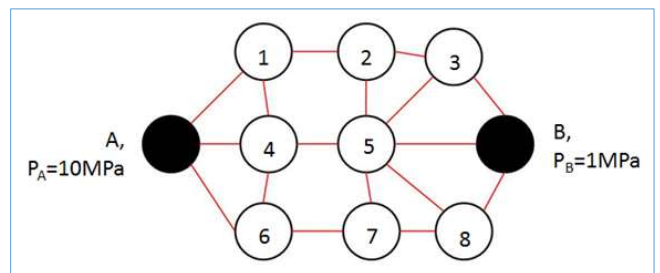


Fig. 2. Pore Network-2

When analyzing the flow of incompressible fluids through porous networks, it becomes essential to establish a set of assumptions that provide a foundation for the modeling process. Firstly, it is assumed that the system operates under ideal conditions where there is neither energy loss nor energy production. This assumption ensures that the energy balance within the system remains constant, facilitating a simplified analysis of fluid flow dynamics. Additionally, the absence of any sink or source of mass within the system ensures a steady-state flow regime, where the mass of the fluid remains constant over time, further simplifying the analysis.

Another critical assumption made in the modeling process is the characterization of pore throats within the network as uniform tubes. This simplification allows for the representation of the complex pore structure as a series of uniform channels, with each throat having the same dimensions in terms of radius and length. By treating pore throats as uniform tubes, the geometric complexities associated with irregular pore structures are mitigated, enabling a more straightforward analysis of fluid flow behavior.

Furthermore, it is assumed that the fluid properties such as temperature, density, and viscosity remain uniform throughout the entire system. This assumption ensures that the fluid behaves consistently across the porous network, simplifying the modeling process. For example, when

considering the flow of methane at 300 K, it is assumed that the fluid maintains constant density and viscosity properties, regardless of its location within the network.

To facilitate comparison with alternate scenarios, density and viscosity values are chosen based on the average pressure within the system. This approach ensures a standardized analysis method, allowing for meaningful comparisons between different scenarios. These assumptions collectively provide a framework for modeling fluid flow through porous networks, enabling researchers to systematically examine flow behavior and performance in various industrial applications. Mass balance can be set up for each pore using Hagen-Poiseuille equation, with flux/ flow rate associated with each pore should be zero at steady state.

Mass flow rate between pore-i and pore-j:

$$W_{ij} = \frac{\pi r^4 \rho (P_i - P_j)}{8 \mu L} \text{ (flow from i to j as positive)} \quad (1)$$

where;

$$r = 20 \times 10^{-9} \text{ m};$$

$$L = 150 \times 10^{-9} \text{ m};$$

$$\rho = 39.5973 \text{ kg/m}^3;$$

$$\mu = 1.21316 \times 10^{-5} \text{ Pa} \cdot \text{S}$$

### 3.1. For Network 1

Since we have constant cross section for each pore throat, mass balance at steady state can be set up as following:

$$\text{pore \#1: } W_{1A} + W_{12} = 0 \quad (2)$$

$$\text{pore \#2: } W_{21} + W_{23} = 0 \quad (3)$$

$$\text{pore \#3: } W_{32} + W_{3B} = 0 \quad (4)$$

$$\text{pore \#4: } W_{4A} + W_{45} = 0 \quad (5)$$

$$\text{pore \#5: } W_{5A} + W_{5B} = 0 \quad (6)$$

$$\text{pore \#6: } W_{6A} + W_{67} = 0 \quad (7)$$

$$\text{pore \#7: } W_{76} + W_{78} = 0 \quad (8)$$

$$\text{pore \#8: } W_{87} + W_{8B} = 0 \quad (9)$$

Boundary conditions:

$$P_A = 10 \times 10^6 \text{ Pa} \quad (10)$$

$$P_B = 1 \times 10^6 \text{ Pa} \quad (11)$$

Then we can solve the above Equations from (1) to (11) to get the pressure distribution in network, and then flow rate in the network can be obtained with Hagen-Poiseuille equation.

The results are discussed together with results for network2. To solve the systems of linear equations, we use matrix calculation  $X=A \setminus b$  method in matlab, and matrix A in both networks are nonsingular.

### 3.2. For Network 2

Similarly, we can set up mass balance for network 2 as follows:

$$\text{pore \#1: } W_{1A} + W_{12} + W_{14} = 0 \quad (12)$$

$$\text{pore \#2: } W_{21} + W_{25} + W_{23} = 0 \quad (13)$$

$$\text{pore \#3: } W_{32} + W_{3B} + W_{35} = 0 \quad (14)$$

$$\text{pore \#4: } W_{4A} + W_{41} + W_{45} + W_{46} = 0 \quad (15)$$

$$\text{pore \#5: } W_{5A} + W_{52} + W_{53} + W_{5B} + W_{58} + W_{57} = 0 \quad (16)$$

$$\text{pore \#6: } W_{6A} + W_{64} + W_{67} = 0 \quad (17)$$

$$\text{pore \#7: } W_{76} + W_{75} + W_{78} = 0 \quad (18)$$

$$\text{pore \#8: } W_{87} + W_{85} + W_{8B} = 0 \quad (19)$$

Boundary conditions:

$$P_A = 10 \times 10^6 \text{ Pa} \quad (20)$$

$$P_B = 1 \times 10^6 \text{ Pa} \quad (21)$$

Again, we can solve Equations 1, 12-21 to get the pressure distribution and then acquire the flow rate in the network. The same numerical method can be applied for the calculation as for network1.

## 4. Results and Discussion

Furthermore, to provide a comprehensive analysis of the fluid flow within the porous network, detailed data regarding pressure distribution and flow distribution are presented below in Tables 1 and 2, respectively.

Table 1 – Pressure distribution

Pore	P <sub>i</sub> (Mpa)	
	Network1	Network2
#1	7.7500	7.4110
#2	5.5000	4.9863
#3	3.2500	3.3836
#4	7.0000	7.2466
#5	4.0000	4.1644
#6	7.7500	7.4110
#7	5.5000	4.9863
#8	3.2500	3.3836

These tables offer valuable insights into the spatial variation of flow rates and pressure gradients within the system, enabling a more thorough understanding of fluid behavior in complex porous media configurations. By examining these datasets alongside the established assumptions, researchers

can gain a deeper insight into the underlying mechanisms governing fluid flow dynamics and pressure behavior in porous networks.

Table 2 – Flow rate distribution

Pore	Associated pore throat rate $W_{ij}$ (Kg/s)	Network 1	Network 2	
#1	$W_{1A}$	-3.0747e-012	-3.5380e-012	
	$W_{12}$	3.0747e-012	3.3133e-012	
	$W_{14}$	N.A.	2.2463e-013	
$W_1$ (total flow rate for pore #1)		-0.3635 e-026 << $W_{ij}$	0.7699 e-026 << $W_{ij}$	
#2	$W_{21}$	-3.0747e-012	-3.3133e-012	
	$W_{23}$	3.0747e-012	2.1902e-012	
	$W_{25}$	N.A.	1.1232e-012	
#3	$W_2$	e-026 << $W_{ij}$	-0.5049 e-026 << $W_{ij}$	
	$W_{32}$	-3.0747e-012	-2.1902e-012	
	$W_{3B}$	3.0747e-012	3.2572e-012	
#4	$W_3$	0.3635 e-026 << $W_{ij}$	-0.1818 e-026 << $W_{ij}$	
	$W_{4A}$	-4.0996e-012	-3.7626e-012	
	$W_{41}$	N.A.	-2.2463e-013	
#5	$W_{45}$	4.0996e-012	4.2119e-012	
	$W_{46}$	N.A.	-2.2463e-013	
	$W_4$	-0.1212 e-026 << $W_{ij}$	-0.9744 e-026 << $W_{ij}$	
#6	$W_{54}$	-4.0996e-012	-4.2119e-012	
	$W_{5B}$	4.0996e-012	4.3242e-012	
	$W_{52}$	N.A.	-1.1232e-012	
#7	$W_{53}$	N.A.	1.0670e-012	
	$W_{58}$	N.A.	1.0670e-012	
	$W_{57}$	N.A.	-1.1232e-012	
#8	$W_5$	-0.4847 e-026 << $W_{ij}$	-0.4645 e-026 << $W_{ij}$	
	$W_{6A}$	-3.0747e-012	-3.5380e-012	
	$W_{67}$	3.0747e-012	3.3133e-012	
#9	$W_{64}$	N.A.	2.2463e-013	
	$W_6$	0.2423 e-026 << $W_{ij}$	-0.6033 e-026 << $W_{ij}$	
	$W_{76}$	-3.0747e-012	-3.3133e-012	
#10	$W_{78}$	3.0747e-012	2.1902e-012	
	$W_{75}$	N.A.	1.1232e-012	
	$W_7$	-0.3635 e-026 << $W_{ij}$	-0.1414 e-026 << $W_{ij}$	
#11	$W_{87}$	-3.0747e-012	-2.1902e-012	
	$W_{8B}$	3.0747e-012	3.2572e-012	
	$W_{85}$	N.A.	-1.0670e-012	
#12	$W_8$	0.3635 e-026 << $W_{ij}$	0 e-026 << $W_{ij}$	
	Total	$W_{tot}=W_A=W_B$	<b>1.0250e-011</b>	<b>1.0839e011</b>

Total flow rate:

Network 1:  $W_{total}=1.0250 e-11$  kg/s

Network 2:  $W_{total}= 1.0839 e-11$  kg/s

The distribution of pressure and flow rate is shown graphically as bellow:

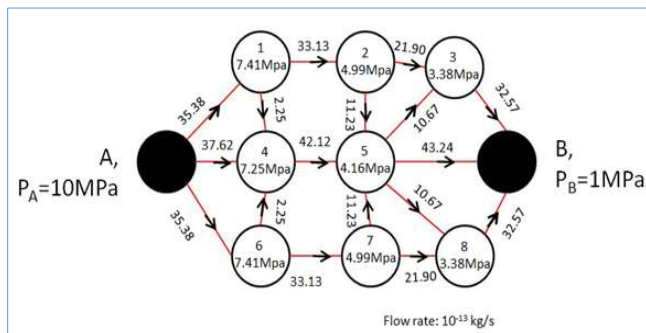


Fig. 3. Pressure and flow rate distribution in Network 1

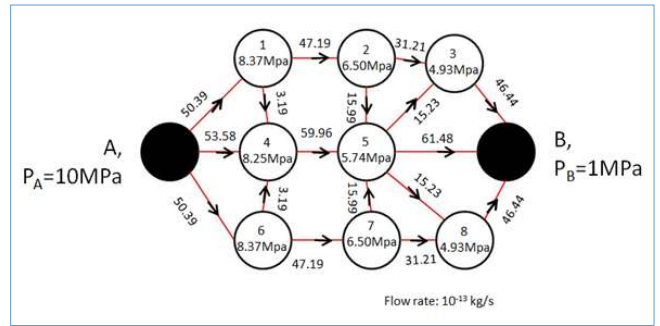


Fig. 4. Pressure and flow rate distribution in Network 2

From the above distribution, we see the main differences between network1 and network 2:

Network1 has three independent paths (1-2-3; 4-5; 6-7-8), each path can be treated as a pipe with constant cross section and the flow rate in each path is proportional the pressure gradient; The flow and pressure are independent on flow and pressure in other paths, since they are not connected. However, network2 has each path connected to each other, the pressure and flow rate of each path receives “regulation” because of this interconnection. The total flow rate of network1 is slightly smaller than the total flow rate in network2, this is partly due to the interconnection among pores increases the “effective cross section area”.

### 5. Conclusion

In conclusion, this study has provided valuable insights into the dynamics of fluid flow and pressure distribution within porous networks. By employing a series of carefully crafted assumptions and computational modeling techniques, we have been able to analyze the behavior of incompressible fluids flowing through pore throats with greater clarity. The assumptions, ranging from the uniformity of pore throat dimensions to the constant fluid properties throughout the system, have allowed us to simplify the complexity of porous media and focus on fundamental fluid behavior principles. The presented data in Tables 1 and 2 offer detailed insights into the flow distribution and pressure gradients within the system, highlighting the spatial variations and providing a basis for further analysis.

Through this study, we have demonstrated the importance of computational modeling in understanding fluid behavior in porous media and its implications for various industrial applications. While our assumptions provide a framework for analysis, it is essential to recognize their limitations and consider the potential impact of deviations from these idealized conditions in real-world scenarios. Future research could explore the effects of varying pore throat geometries, non-uniform fluid properties, and transient flow conditions to further refine our understanding of fluid flow dynamics in porous media and lays the groundwork for future investigations in this field.

### References

Alagoz, E., 2023. Development and Analysis of a Program for

- Phase-Equilibrium Calculations Using the Peng-Robinson Equation of State. International Journal of Earth Sciences Knowledge and Applications 5 (1), 51-61.
- Alagoz, E., Giozza, G.G., 2023. Calculation of Bottomhole Pressure in Two-Phase Wells Using Beggs and Brill Method: Sensitivity Analysis. International Journal of Earth Sciences Knowledge and Applications 5 (3) 333-337.
- Alagoz, E., Mengen, A.E., Bensenouci, F., Dundar, E.C., 2023. Computational Tool for Wellbore Stability Analysis and Mud Weight Optimization v1.0. International Journal of Current Research Science Engineering Technology 7 (1), 1-5.
- Jones, D., Smith, A., 2019. Surface roughness effects on pressure dynamics in pore throats: Insights from experimental and modeling studies. Journal of Applied Physics 125(15), 155901.
- Smith, A., Johnson, B., 2018. Understanding pressure dynamics in porous media: Insights from pore structure analysis. Journal of Porous Materials 15(3), 301-315.
- Wang, C. et al., 2020. Visualization of pressure distribution in porous media using X-ray microtomography. Geophysical Research Letters 47 (7), e2020GL089135.

## Appendices

### Calculation Explanation

Table 3 – MATLAB Codes Explanation

Matlab Programm	Purpose
Senario_a_1.m	Calculate pressure and flow rate distribution in network 1 using $x=A \setminus b$ method
Senario_a_2.m	Calculate pressure and flow rate distribution in network 2 using $x=A \setminus b$ method

### Senario a 1.m MATLAB CODES

```
% Senario a) Network1
% parameters
r= 20*10^(-9); L=150*10^(-9);
rou= 39.5973; miu= 1.21316*10^(-5); P_A=10;P_B=1; epsilon=1.0e-20;

% system of linear equations for mass balance in terms of pressure
A=[2 -1 0 0 0 0 0 0;
-1 2 -1 0 0 0 0 0;
0 -1 2 0 0 0 0 0;
0 0 0 2 -1 0 0 0;
0 0 0 -1 2 0 0 0;
0 0 0 0 0 2 -1 0;
0 0 0 0 0 -1 2 -1;
0 0 0 0 0 0 -1 2;
];
b=[10;0;1;10;1;10;0;1;];

% check matrix A single or not
C=det(A);
str = sprintf('det(A)= %d', C);
disp(str);
if abs(C) < epsilon, error('A is singular matrix!');
break;
end;

% solve pressure distribution from above
% system of linear equations by matrix
P=A \ b

% flow rate of pore #1
W_1A= 3.14*r^4*rou/(8*miu*L)*(P(1)-P_A)*10^6
W_12= 3.14*r^4*rou/(8*miu*L)*(P(1)-P(2))*10^6
% flow rate of pore #2
W_21= 3.14*r^4*rou/(8*miu*L)*(P(2)-P(1))*10^6
W_23= 3.14*r^4*rou/(8*miu*L)*(P(2)-P(3))*10^6
% flow rate of pore #3
W_32= 3.14*r^4*rou/(8*miu*L)*(P(3)-P(2))*10^6
W_3B= 3.14*r^4*rou/(8*miu*L)*(P(3)-P_B)*10^6
```

```

% flow rate of pore #4
W_4A= 3.14*r^4*rou/(8*miu*L)*(P(4)-P_A)*10^6
W_4B= 3.14*r^4*rou/(8*miu*L)*(P(4)-P(5))*10^6
% flow rate of pore #5
W_5A= 3.14*r^4*rou/(8*miu*L)*(P(5)-P(4))*10^6
W_5B= 3.14*r^4*rou/(8*miu*L)*(P(5)-P_B)*10^6
% flow rate of pore #6
W_6A= 3.14*r^4*rou/(8*miu*L)*(P(6)-P_A)*10^6
W_6B= 3.14*r^4*rou/(8*miu*L)*(P(6)-P(7))*10^6
% flow rate of pore #7
W_7A= 3.14*r^4*rou/(8*miu*L)*(P(7)-P(6))*10^6
W_7B= 3.14*r^4*rou/(8*miu*L)*(P(7)-P(8))*10^6
% flow rate of pore #8
W_8A= 3.14*r^4*rou/(8*miu*L)*(P(8)-P(7))*10^6
W_8B= 3.14*r^4*rou/(8*miu*L)*(P(8)-P_B)*10^6

```

```

% check balance of flow rate

```

```

W(1)=W_1A+W_12;
W(2)=W_21+W_23;
W(3)=W_32+W_3B;
W(4)=W_4A+W_45;
W(5)=W_54+W_5B;
W(6)=W_6A+W_67;
W(7)=W_76+W_78;
W(8)=W_87+W_8B;

```

```

%Display total flow rate for each pore

```

```

W
W_total=W_1A+W_4A+W_6A

```

### **Senario a 2.m MATLAB CODES**

```

% Senario a) Network2
% parameters
r= 20*10^(-9); L=150*10^(-9);
rou= 39.5973; miu= 1.21316*10^(-5); P_A=10;P_B=1;epsilon=1.0e-20;

```

```

% system of linear equations for mass balance in terms of pressure

```

```

A=[
 3 -1 0 -1 0 0 0 0 ;
-1 3 -1 0 -1 0 0 0 ;
 0 -1 3 0 -1 0 0 0 ;
-1 0 0 4 -1 -1 0 0 ;
 0 -1 -1 -1 6 0 -1 -1;
 0 0 0 -1 0 3 -1 0;
 0 0 0 0 -1 -1 3 -1;
 0 0 0 0 -1 0 -1 3;
];
b=[10;0;1;10;1;10;0;1;];

```

```

% check matrix A single or not

```

```

C=det(A);
str = sprintf('det(A)= %d', C);
disp(str);
if abs(C) < epsilon, error('A is singular matrix!');
break;
end;

```

```

% solve pressure distribution from above

```

```

%system of linear equations by matrix
P=A\b

```

```

% flow rate of pore #1

```

$$W_{1A} = 3.14 * r^4 * rou / (8 * miu * L) * (P(1) - P_A) * 10^6$$

$$W_{12} = 3.14 * r^4 * rou / (8 * miu * L) * (P(1) - P(2)) * 10^6$$

$$W_{14} = 3.14 * r^4 * rou / (8 * miu * L) * (P(1) - P(4)) * 10^6$$

% flow rate of pore #2

$$W_{21} = 3.14 * r^4 * rou / (8 * miu * L) * (P(2) - P(1)) * 10^6$$

$$W_{23} = 3.14 * r^4 * rou / (8 * miu * L) * (P(2) - P(3)) * 10^6$$

$$W_{25} = 3.14 * r^4 * rou / (8 * miu * L) * (P(2) - P(5)) * 10^6$$

% flow rate of pore #3

$$W_{32} = 3.14 * r^4 * rou / (8 * miu * L) * (P(3) - P(2)) * 10^6$$

$$W_{3B} = 3.14 * r^4 * rou / (8 * miu * L) * (P(3) - P_B) * 10^6$$

$$W_{35} = 3.14 * r^4 * rou / (8 * miu * L) * (P(3) - P(5)) * 10^6$$

% flow rate of pore #4

$$W_{4A} = 3.14 * r^4 * rou / (8 * miu * L) * (P(4) - P_A) * 10^6$$

$$W_{41} = 3.14 * r^4 * rou / (8 * miu * L) * (P(4) - P(1)) * 10^6$$

$$W_{45} = 3.14 * r^4 * rou / (8 * miu * L) * (P(4) - P(5)) * 10^6$$

$$W_{46} = 3.14 * r^4 * rou / (8 * miu * L) * (P(4) - P(6)) * 10^6$$

% flow rate of pore #5

$$W_{54} = 3.14 * r^4 * rou / (8 * miu * L) * (P(5) - P(4)) * 10^6$$

$$W_{5B} = 3.14 * r^4 * rou / (8 * miu * L) * (P(5) - P_B) * 10^6$$

$$W_{52} = 3.14 * r^4 * rou / (8 * miu * L) * (P(5) - P(2)) * 10^6$$

$$W_{53} = 3.14 * r^4 * rou / (8 * miu * L) * (P(5) - P(3)) * 10^6$$

$$W_{58} = 3.14 * r^4 * rou / (8 * miu * L) * (P(5) - P(8)) * 10^6$$

$$W_{57} = 3.14 * r^4 * rou / (8 * miu * L) * (P(5) - P(7)) * 10^6$$

% flow rate of pore #6

$$W_{6A} = 3.14 * r^4 * rou / (8 * miu * L) * (P(6) - P_A) * 10^6$$

$$W_{67} = 3.14 * r^4 * rou / (8 * miu * L) * (P(6) - P(7)) * 10^6$$

$$W_{64} = 3.14 * r^4 * rou / (8 * miu * L) * (P(6) - P(4)) * 10^6$$

% flow rate of pore #7

$$W_{76} = 3.14 * r^4 * rou / (8 * miu * L) * (P(7) - P(6)) * 10^6$$

$$W_{75} = 3.14 * r^4 * rou / (8 * miu * L) * (P(7) - P(5)) * 10^6$$

$$W_{78} = 3.14 * r^4 * rou / (8 * miu * L) * (P(7) - P(8)) * 10^6$$

% flow rate of pore #8

$$W_{87} = 3.14 * r^4 * rou / (8 * miu * L) * (P(8) - P(7)) * 10^6$$

$$W_{85} = 3.14 * r^4 * rou / (8 * miu * L) * (P(8) - P(5)) * 10^6$$

$$W_{8B} = 3.14 * r^4 * rou / (8 * miu * L) * (P(8) - P_B) * 10^6$$

% check balance of flow rate

$$W(1) = W_{1A} + W_{12} + W_{14};$$

$$W(2) = W_{21} + W_{23} + W_{25};$$

$$W(3) = W_{32} + W_{3B} + W_{35};$$

$$W(4) = W_{4A} + W_{45} + W_{41} + W_{46};$$

$$W(5) = W_{54} + W_{5B} + W_{52} + W_{53} + W_{58} + W_{57};$$

$$W(6) = W_{6A} + W_{67} + W_{64};$$

$$W(7) = W_{76} + W_{78} + W_{75};$$

$$W(8) = W_{87} + W_{8B} + W_{85};$$

%Display total flow rate for each pore

$$W$$

$$W_{total} = W_{1A} + W_{4A} + W_{6A}$$

### **Flux.m MATLAB CODES**

```
function J = flux(P1,P2)
r= 20*10^(-9); M=16.04*10^-3; R=8.314; T=300; L=150*10^(-9);
miu= 1.1242*10^(-5); rou0= 6.57281; p0=1; alpha=0.8;
Tc=191.15; Pc=4.641*10^6; omega=0.0115;
```

```

P_avg =(P1+P2)/2;

% caclulate compressibility factor Z
Tr=T/Tc;
k=0.37466+1.54226*omega-0.26992*omega^2;
a=0.457235*8.314^2*Tc^2/Pc;
b=0.077796*8.314*Tc/Pc;
alpha_0=(1+k*(1-Tr^0.5))^2;
A=a*alpha_0*P_avg*10^6/(8.314^2*300^2);
B=b*P_avg*10^6/(8.314*300);
Q=[1,B-1,A-2*B-3*B*B,-(A*B-B^2-B^3)];
z_temp=roots(Q);
Z=max(z_temp);

% calculate average density
rou_avg=P_avg*(10^6)*M/R/T/Z;

%calculate F
F = 1 + (8*3.14*R*T/M)^(0.5)*miu*(2/alpha-1)/(P_avg*10^(6)*r);

%calculate flux J
AA = 2*r*M/(3000*R*T);
BB = (8*R*T/(3.14*M))^0.5;
J = -(AA*BB+ F*r^(2)*rou_avg/(8*miu))*(P2-P1)*10^(6)/L;

```

**Output of *Senario a 1.m* MATLAB CODES :**

det(A)= 4.800000e+001

P =

```

7.7500
5.5000
3.2500
7.0000
4.0000
7.7500
5.5000
3.2500

```

```

W_1A = -3.0747e-012
W_12 = 3.0747e-012
W_21 = -3.0747e-012
W_23 = 3.0747e-012
W_32 = -3.0747e-012
W_3B = 3.0747e-012
W_4A = -4.0996e-012
W_45 = 4.0996e-012
W_54 = -4.0996e-012
W_5B = 4.0996e-012
W_6A = -3.0747e-012
W_67 = 3.0747e-012
W_76 = -3.0747e-012
W_78 = 3.0747e-012
W_87 = -3.0747e-012
W_8B = 3.0747e-012
W = 1.0e-026 *
Columns 1 through 7
-0.3635 0.3635 -0.1212 -0.4847 0.2423 -0.3635 0.3635
Column 8
-0.1212
W_total = -1.0249e-011

```

**Output of *Senario a 2.m* MATLAB CODES :**

det(A)= 4599

P =

7.4110  
4.9863  
3.3836  
7.2466  
4.1644  
7.4110  
4.9863  
3.3836

W\_1A = -3.5380e-012

W\_12 = 3.3133e-012

W\_14 = 2.2463e-013

W\_21 = -3.3133e-012

W\_23 = 2.1902e-012

W\_25 = 1.1232e-012

W\_32 = -2.1902e-012

W\_3B = 3.2572e-012

W\_35 = -1.0670e-012

W\_4A = -3.7626e-012

W\_41 = -2.2463e-013

W\_45 = 4.2119e-012

W\_46 = -2.2463e-013

W\_54 = -4.2119e-012

W\_5B = 4.3242e-012

W\_52 = -1.1232e-012

W\_53 = 1.0670e-012

W\_58 = 1.0670e-012

W\_57 = -1.1232e-012

W\_6A = -3.5380e-012

W\_67 = 3.3133e-012

W\_64 = 2.2463e-013

W\_76 = -3.3133e-012

W\_75 = 1.1232e-012

W\_78 = 2.1902e-012

W\_87 = -2.1902e-012

W\_85 = -1.0670e-012

W\_8B = 3.2572e-012

W = 1.0e-026 \*

Columns 1 through 7

0.7699 -0.5049 -0.1818 -0.9744 -0.4645 -0.6033 -0.1414

Column 8

0

W\_total = -1.0839e-011